MOCVD of crystalline Bi_2O_3 thin films using a single-source bismuth alkoxide precursor and their use in photodegradation of water

Savio J. A. Moniz, Christopher S. Blackman,* Claire J. Carmalt, and Geoffrey Hyett

Materials Chemistry Centre, Department of Chemistry, University College London, 20 Gordon Street, London
5 *WC1H 0AJ, UK.*

Email: c.blackman@ucl.ac.uk, Tel: +44(0)2076794703

Received (in XXX, XXX) Xth XXXXXXXXX 200X, Accepted Xth XXXXXXXXX 200X

First published on the web Xth XXXXXXXXX 200X

DOI: 10.1039/b000000x

10

Bismuth (III) *tert*-butoxide [Bi(O^{t}Bu)$_3$] was utilised as a single-source precursor to controllably deposit thin films of different phases of bismuth oxide (Bi_2O_3) on glass substrates via low–pressure chemical vapour deposition (LPCVD). Band gaps for the different phases have been measured (E_g = 2.3 – 3.0 eV) and the films displayed excellent photodegradation of water under near-UV irradiation.

15 **Introduction**

Bismuth oxide (Bi_2O_3) is an important component of several ferroelectric,[1] multiferroic[2,3] and superconducting oxide materials.[4] It has also received much interest due to its use as an ion conducting electrolyte material in solid oxide fuel cells,[5] an electrode material in discriminating gas sensors[6] and as an effective UV light photocatalyst.[7,8] There are a number of distinct crystallographic phases (α, β, γ, δ, ω) of Bi_2O_3 that have been
20 reported; the low temperature α- and high temperature δ- phases are stable whilst the others are metastable.[9]

There is a driving force for the investigation of new cheap, clean and reliable energy sources that have limited environmental impact to meet global demand for energy. Solar energy, in conjunction with a photocatalyst, may be used in order to generate a chemical fuel source (hydrogen) via photochemical reduction of water. The most common materials used for photochemical water splitting are transition metal oxides with d^0 electron
25 configurations, i.e. TiO_2, whose band-gaps (typically 3.0 eV and above) are too high to serve as efficient water splitting photocatalysts under solar irradiation. Bi_2O_3 possesses band-gap values of 2.29 – 3.31 eV depending on the crystalline phase; the optical gap of BiO has been determined to be as high as 3.31 eV, α-Bi_2O_3 to be 2.85 eV[11] and the amorphous phase as low as 2.0 eV).[9] These values indicate the potential of Bi_2O_3 to serve as a photocatalyst under solar irradiation, and the photocatalytic activities of undoped α- β- and δ-Bi_2O_3 have been
30 demonstrated during degradation of model pollutant dyes Rhodamine B[7,10] and methylene orange,[11] whilst transition metal doped γ-Bi_2O_3 nanoparticles have been shown to photocatalytically split water.[8]

Bismuth oxide films have previously been grown by CVD in dual-source reactions with oxygen and triphenylbismuth, [Bi(C_6H_5)$_3$]. [Bi(C_6H_5)$_3$] is the most commonly used CVD precursor due to its low air and moisture sensitivity[12] and it has been the subject of numerous studies concerning its deposition characteristics

and mechanism of transport in the gas phase using in-situ FTIR spectroscopy.[13] Similarly [Bi(o-tol)$_3$] and [Bi(p-tol)$_3$] have been shown to be useful bismuth precursors for growth of bismuth oxide films.[14] However, the high thermal stability of these precursors requires high deposition temperatures and carbon contamination can be problematic. Trimethylbismuth has been shown to deposit α-Bi_2O_3 films in a dual source reaction with oxygen,[15,16] however trimethylbismuth is pyrophoric and requires cooling prior to and during deposition.

In general, the availability of volatile single-source bismuth oxide precursors for CVD is extremely limited. To overcome the problems of precursor volatility and high deposition temperatures new single-source precursors are required to deposit phase-pure Bi_2O_3 films. The basic requirements for incorporation of oxygen into the molecule using sterically bulky ligands to limit oligomerisation have led to the development of three main types of oxygen-containing precursor:

Alkoxides, [M(OR)$_3$], R = alkyl, aryl, OR (donor functionalised), CX_3 (X = halogen)

Beta-diketonates, [M(R^1COCHCOR^2)$_3$], R = alkyl, aryl, CX_3 (X = halogen)

Carboxylates, [M(O_2CR)$_3$], R = alkyl, aryl, CX_3 (X = halogen)

Alkoxides of bismuth appear to exhibit a common problem of poor solubility and poor volatility and to date there appears to be only two bismuth alkoxides in the literature that have been used for CVD. [Bi(OCMe_2Et)$_3$] and [Bi(OCMe_2CH_2OMe)$_3$] (also known as [Bi(mmp)$_3$]) have both been used as the bismuth source for deposition of $SrBi_2Ta_2O_9$ films. Jones and co-workers reported the crystal structure of [Bi(mmp)$_3$] as monomeric and gave a description of its use in the MOCVD of bismuth oxide with oxygen as the reactive gas using Direct Liquid Injection CVD (DLI-CVD).[17] The use of [Bi(O^{t}Bu)$_3$] has been suggested for Atomic Layer Deposition (ALD) of bismuth oxide but proved unsuccessful in this methodology.[18]

Similarly, there is little mention of the use of bismuth β-diketonates for CVD and the most common example is that of bismuth tetramethylheptanedionate, ([Bi(thd)$_3$] or [Bi(dpm)$_3$]), which has a lower decomposition temperature than alkylbismuth and bismuth halide compounds, but possesses poor thermal stability upon sublimation. Kang[19] used DLI-CVD of [Bi(thd)$_3$] to deposit amorphous Bi_2O_3 on silicon substrates at temperatures between 240-435 °C, using an oxygen gas co-reactant.

Bismuth silyl amide [Bi(N(SiMe_3)$_2$]$_3$ has been used in conjunction with H_2O to produce BiO_x films via Atomic Layer Deposition (ALD).[20] The ease of synthesis, excellent solubility and relative ease of sublimation of [Bi(N(SiMe_3)$_2$]$_3$ led to its use as an ALD precursor, however poor reproducibility in deposition of the binary oxide phase was encountered. It was also suggested that the use of more reactive di-oxygen instead of H_2O would lead to deposition of bismuth silicate films.

In all examples of CVD of crystalline Bi_2O_3 films, oxygen gas or plasma was required during depositions; the use of $[Bi(mmp)_3]$ as a single-source precursor has been briefly mentioned, but no details regarding crystalline phase(s) obtained were given in the paper.[17]

We have investigated the decomposition characteristics of $[Bi(O^tBu)_3]$, $[Bi(mmp)_3]$ and $[Bi(thd)_3]$ by coupled
5 mass spectrometry–thermal gravimetric analysis–differential scanning calorimetry (MS-TGA-DSC) in order to identify suitable deposition conditions and to understand the decomposition pathway of the precursors. The sublimation characteristics of $[Bi(O^tBu)_3]$ suggest that it is suitably volatile at relatively mild temperatures and pressures to be used as a solid-state precursor for LPCVD, with the sterically demanding O^tBu groups inhibiting oligomerization, enhancing volatility (it has been shown to be monomeric in the gas phase)[21] and the
10 decomposition characteristics indicate clean decomposition to Bi_2O_3. We present the first use of a single-source bismuth alkoxide precursor, $[Bi(O^tBu)_3]$, for phase selective deposition of crystalline Bi_2O_3 thin films using LPCVD, utilising a range of substrate temperatures, system pressures and carrier gas flow rates. The films obtained were fully characterised, and we have investigated for the first time, Bi_2O_3 films grown by CVD for photodegradation of water.

15

EXPERIMENTAL

General Procedures

All reactions were performed under a dry, oxygen-free nitrogen atmosphere using standard Schlenk techniques and an Mbraun Unilab glove box. Nitrogen (99.96%) was obtained from BOC and used as supplied. All
20 reagents were used without further purification, and were procured from Sigma Aldrich or Alfa Aesar Ltd. CVD experiments were performed using a horizontal cold wall CVD reactor which has previously been detailed elsewhere.[22] The pressure of the reactor and inlet gas flows were regulated using mechanical throttle valves. Nitrogen was used as a carrier gas. The substrate temperature was varied between 425 – 500 °C, and the bubbler temperature maintained at 110 °C. Depositions were carried out for 1 h on 30 mm x 15 mm borosilicate
25 glass slides, and approximately 150 mg of fresh precursor was used for each deposition.

Physical Measurements

Coupled mass spectrometry – thermal gravimetric analysis – differential scanning calorimetry (MS-TGA-DSC) was performed using a Netzsch STA 449C instrument. The TGA was carried out in sealed aluminium pans,
30 pierced with a small hole just prior to analysis, at atmospheric pressure, under a flow of helium gas (50 cm^3/min). The rate of heating was 10 °C min^{-1}. Grazing incidence (5°) powder X-ray diffraction (XRD) was carried out on a Bruker AXS D8 Discover machine using monochromatic Cu-K_α radiation (λ_1 = 1.54 Å), with phase information obtained via the EVA suite of programs (version 2). Scanning electron microscope (SEM) images were obtained on a JSM-6301F Scanning Microscope Field Emission machine after coating samples

with an ultrathin layer of gold (not observed in images) to avoid charging. UV-Vis spectra were recorded in transmission mode over the range 175-2500 nm using a Perkin Elmer Lambda 950 photospectrometer. Raman spectra were acquired using a Renishaw Raman System 1000 using a helium-neon laser wavelength of 515 nm. XPS spectra were obtained using a Kratos AXIS Ultra machine with a Delay line detector. A monochromated
5 Al-K_α X-ray source producing a FWHM on the Ag $3d_{5/2}$ peak of 0.48 eV was used. A chamber pressure of 7 x 10^{-9} torr was maintained during the scans. The samples were earthed using copper clips to prevent charging, and were etched for 10 mins at 4 kV. Spectra were fitted using CasaXPS version 2.3.15. Full width at half maximum (FHWMs) were constrained between 0.9 – 1.3 for Bi 4f, and its peak position constrained between 153.9 – 168 eV. For O 1s, the FWHM was constrained between 1.3 – 1.7 and its position limited between 524.7
10 – 543 eV.

Synthesis

$[Bi(O^tBu)_3]$ was synthesised according to the literature in 82% yield.[18,23] Tris(1-methoxy-2-methyl-2-propanolato)bismuth(III), {$[Bi(mmp)_3]$}, was synthesised according to a literature procedure via an alcohol-
15 amine exchange in 58% yield, and possessed identical ^1H NMR, ^{13}C NMR, infrared and microanalytical data.[17,24] $[Bi(thd)_3]$ was synthesised from a modified version of the literature preparation from $[Bi(N(SiMe_3)_2]_3$ and the free ligand (Hthd) in 76% yield, and possessed identical ^1H NMR, ^{13}C NMR, infrared and microanalytical data to those published.[18,23]

20 **RESULTS**

The decomposition profiles of $[Bi(mmp)_3]$, $[Bi(thd)_3]$ and $[Bi(O^tBu)_3]$ were examined by coupled MS-TGA-DSC under a helium atmosphere (Figure 1).

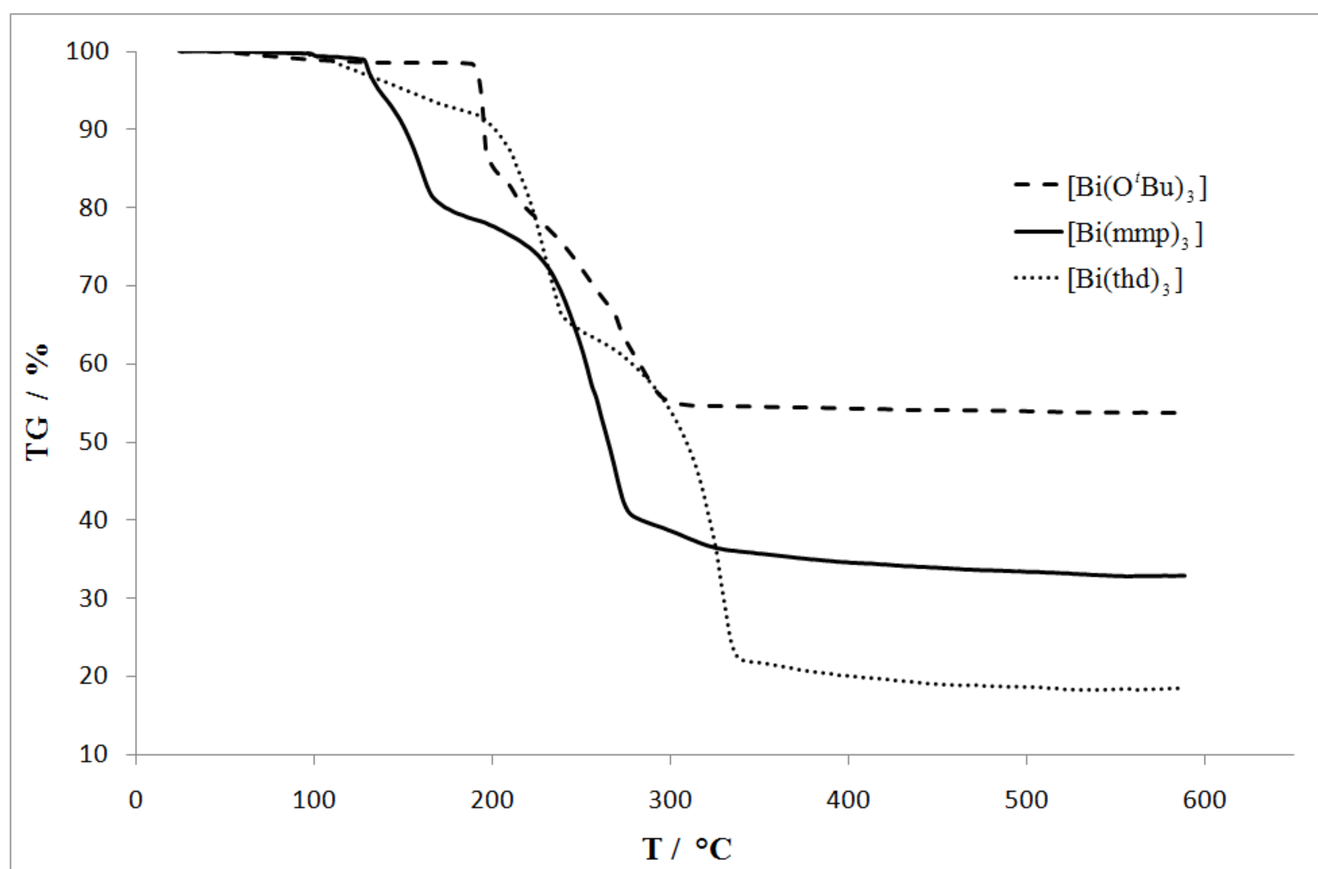

Figure 1 - TGA patterns of $[Bi(mmp)_3]$, $[Bi(thd)_3]$ and $[Bi(O^tBu)_3]$

The TGA data of $[Bi(mmp)_3]$ shows a negligible weight loss (1.1%) up to 129 °C, most likely due to excess
5 solvent molecules remaining after synthesis, and may be ignored. An endotherm is observed in the DSC trace (not shown) at 130 °C, which is assigned as the melting point of $[Bi(mmp)_3]$, and this is followed by the first steep weight loss of 18.3% up to 171 °C which is attributed to volatilisation of the precursor. Subsequent weight loss of 39.8% is observed between 171 and 279 °C, which is coincident with an exotherm in the DSC (not shown) and is therefore attributed to decomposition of the precursor. Between 280 °C and the end of the TGA
10 experiment (600 °C), there was a small weight loss of 7.7%. The fraction of weight loss observed during the decomposition of the precursor is ~ 50% (~40% total mass loss from a total mass of 80%, corrected for sample lost during volatilisation), which is somewhat lower than expected for formation of Bi_2O_3 (55.1% mass loss would equate to the formation of Bi_2O_3), although whether this is due to incomplete precursor decomposition or additional precursor evaporation is unclear, with XRD analysis of the TGA residue not revealing any peaks not
15 assigned to Bi_2O_3.

The TGA data of $[Bi(thd)_3]$ shows a negligible weight loss (1.5%) up to the melt at 113 °C (observed in the DSC trace), possibly due to residual moisture or solvent molecules, and may be ignored. Between 113 °C and 195 °C there is loss of 7.5% of mass, which coincides with the observation of an endotherm in the DSC (not shown) at 113 °C (assigned as the melt) and this is therefore ascribed to volatilisation of the precursor. This is
20 followed by two separate weight loss steps of 26.6% by 246 °C and 46.3% to 600 °C, which coincide with

exotherms in the DSC (not shown) and are therefore due to precursor decomposition. The fraction of weight loss ascribed to precursor decomposition is ~ 80% (~ 73% mass loss from a total mass of 91 % after precursor evaporation), which is not consistent with the formation of Bi_2O_3 only, which requires a mass loss of 69.3%. This additional weight loss may be due to decomposition to metallic bismuth or a suboxide, however the XRD
5 pattern of the residue was complex and neither species could be confirmed from the data.

The TGA data of [Bi(O^{t}Bu)$_3$] shows negligible weight loss (1.70%) up to 189 °C, with an endotherm observed in the DSC trace (not shown) assigned as the melt, hence this weight loss is most likely to volatilisation of the precursor. There then follows a weight loss of 11.0% to 197 °C, which is conincident with an exotherm in the DSC, hence indicating partial decomposition. A second weight loss step of 32.8% to 318 °C is also observed,
10 again coincident with exotherms in the DSC, indicative of decomposition. The fraction of weight loss during precursor decomposition is ~ 45% (~ 44% weight loss from a total mass of 98% after precursor evaporation), which is consistent with the formation of Bi_2O_3 (theoretical mass loss for Bi_2O_3 is 45.7%). During the preparation of this paper TGA data of [Bi(O^{t}Bu)$_3$] was released by researchers investigating the use of this precursor for ALD.[18] In their analysis, when using similar sealed pans to our experiments, they observed thermal
15 decomposition of the precursor by 270 °C, which is consistent with the data reported here allowing for differences in experimental parameters.

Analysis of the decomposition pathways of the three precursors using analysis of the mass loss fragments during each decomposition step and TGA-coupled mass spectrometry did not yield conclusive results with respect to individual precursor decomposition pathways, and as noted XRD analysis of residues was inconclusive, and
20 therefore we are unable to speculate on the cause of the incomplete and excess mass loss in [Bi(mmp)$_3$] and [Bi(thd)$_3$] respectively compared to [Bi(O^{t}Bu)$_3$].

Another important property of a CVD precursor is volatility and the vapour pressures of [Bi(thd)$_3$], [Bi(O^{t}Bu)$_3$] and [Bi(mmp)$_3$] were plotted using vapour pressure equations from the literature (Figure 2).[25,26]

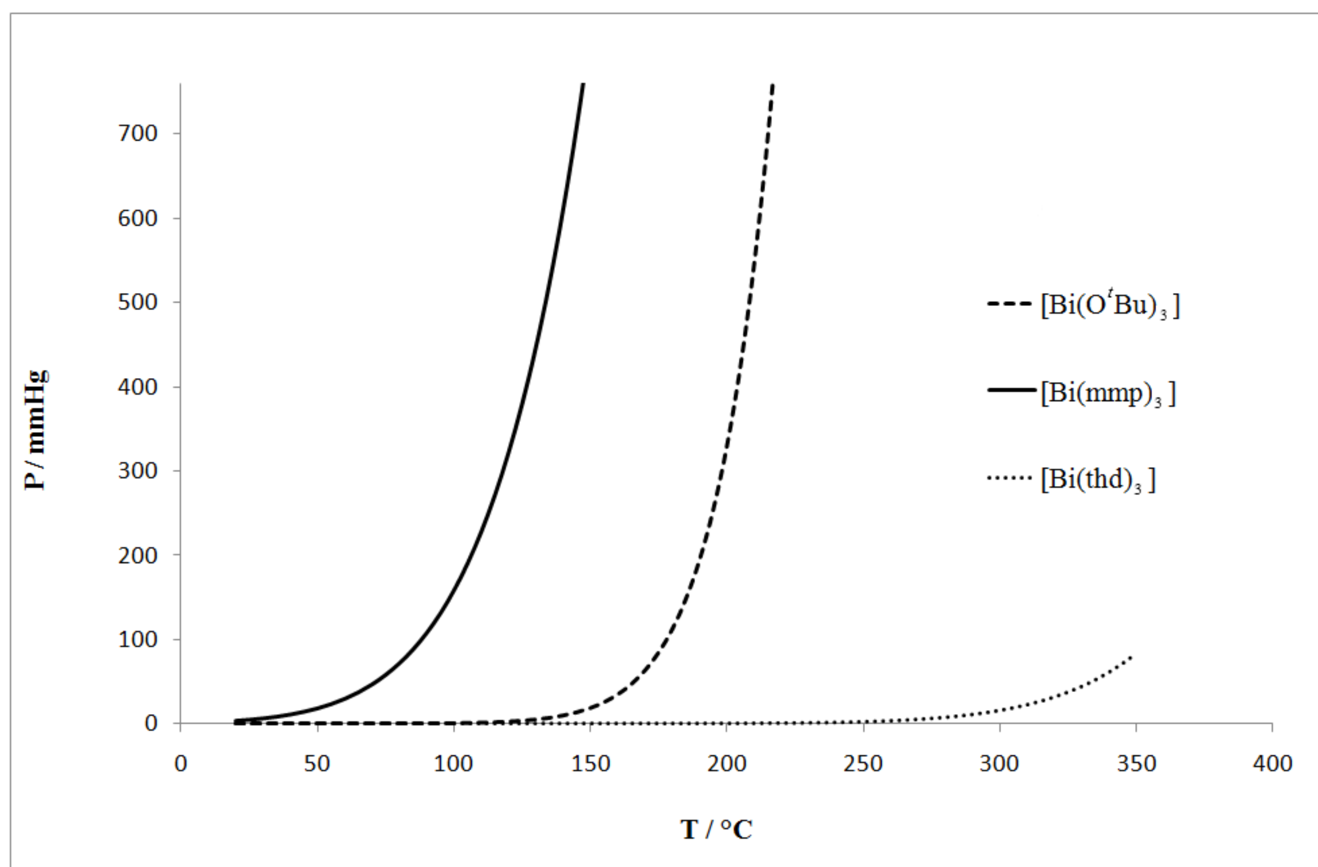

Figure 2 - Vapour pressure curves for [Bi(thd)$_3$], [Bi(O^{t}Bu)$_3$] and [Bi(mmp)$_3$]

[Bi(mmp)$_3$] exhibits a relatively high vapour pressure of 158 mmHg at 100 °C and this correlates with the
5 relatively large mass loss of the precursor (~ 18%) observed in the TGA prior to the onset of decomposition, ascribed to volatilisation. The vapour pressure of [Bi(O^{t}Bu)$_3$] at this temperature is 0.48 mmHg, and is negligible (2.15 x 10^{-4} mmHg) for [Bi(thd)$_3$], which is somewhat surprising given the observed mass loss of 7.5% for the [Bi(thd)$_3$] precursor ascribed to precursor evaporation during TGA analysis. Despite its low vapour pressure, [Bi(thd)$_3$] has been successfully employed as a precursor to Bi_2O_3 films via DLI-CVD,[19] a technique
10 which would assist in overcoming the poor volatility and decomposition characteristics of this precursor.

[Bi(O^{t}Bu)$_3$] exhibits an appreciable vapour pressure that is significantly higher than [Bi(thd)$_3$] and possesses excellent decomposition characteristics for formation of Bi_2O_3, as assessed using TGA, and was therefore selected as the precursor of choice for this study.

CVD

15 The use of [Bi(O^{t}Bu)$_3$] as a single-source precursor to transparent gold/yellow crystalline bismuth oxide thin films was studied over a variety of substrate temperatures (no deposition was obtained below 425 °C), system pressures and carrier gas flow rates. Despite reported decomposition problems encountered when using this precursor for ALD,[18] we did not observe detrimental precursor decomposition when maintaining a bubbler temperature of 110 °C. All films displayed good substrate coverage and were adherent; all films passed the

Scotch tape test but did not survive after treatment with steel wool. The films did not show any changes in characteristics after prolonged storage in air. The CVD growth conditions are shown in Table 1.

Table 1 - Details of the CVD experiments

Substrate temp / °C	Nitrogen flow rate / ccm	System pressure / mbar	Crystalline phase(s)	Film thickness / nm	Bandgap / eV
425	12	8	β	75	2.4
450	12	8	β, γ	302	2.3
475	12	8	β, γ	328	2.3
500	12	8	γ	515	2.8
450	12	15	β, γ	187	2.5
450	12	20	β, γ	294	2.6
450	12	45	α, γ	526	2.8
450	20	8	γ		2.9
450	25	8	γ		2.7
450	40	8	γ		3.0

5

X-ray diffraction patterns revealed the presence of crystalline, mixed phase films, composed of β- and γ- phases. At 500 °C, the γ- phase was the predominant crystalline phase (Figure 3) and this was also the dominant phase upon increasing the carrier gas flow rate from 12 to 40 cm^3/min at 450 °C.

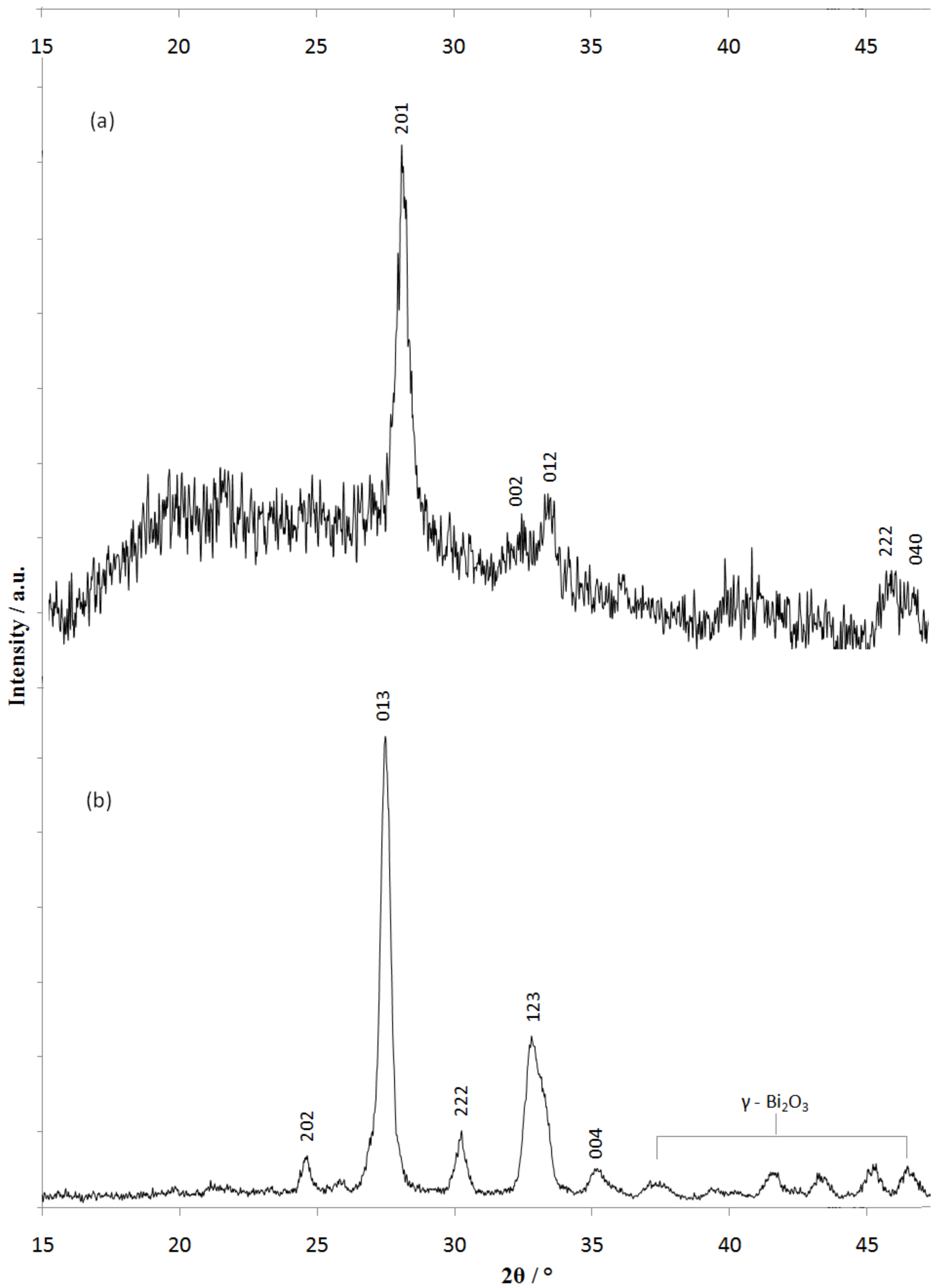

Figure 3- X-Ray diffraction patterns of (a) β-Bi_2O_3 and (b) γ-Bi_2O_3, low intensity peaks not indexed

Unit cell dimensions of $a = b = c = 10.27$ (3) Å obtained for the γ- phase were in agreement with literature values ($a = b = c = 10.25$ Å).[27] At 425 °C (8 mbar), the β- phase was the dominant crystalline species with unit cell dimensions of $a = b = 7.8$ (1) Å, $c = 5.7$ (2) Å for the β- phase in agreement with literature values ($a = b = 7.738$ Å, c = 5.731 Å),[27] and films deposited at 450 and 475 °C resulted in mixed β- and γ- phases. At a carrier gas flow rate of 45 cm^3/min a mixed α- and β- phase was observed. Similar variations in crystalline phases obtained via MOCVD of Bi_2O_3 were also observed by Tondello[12] using triphenylbismuth in a dual-source reaction with oxygen.

Film thickness data were obtained using side-on SEM imaging. As expected, the film growth rate increased as a function of substrate temperature (Figure 4), and also as a function of carrier gas flow rate.

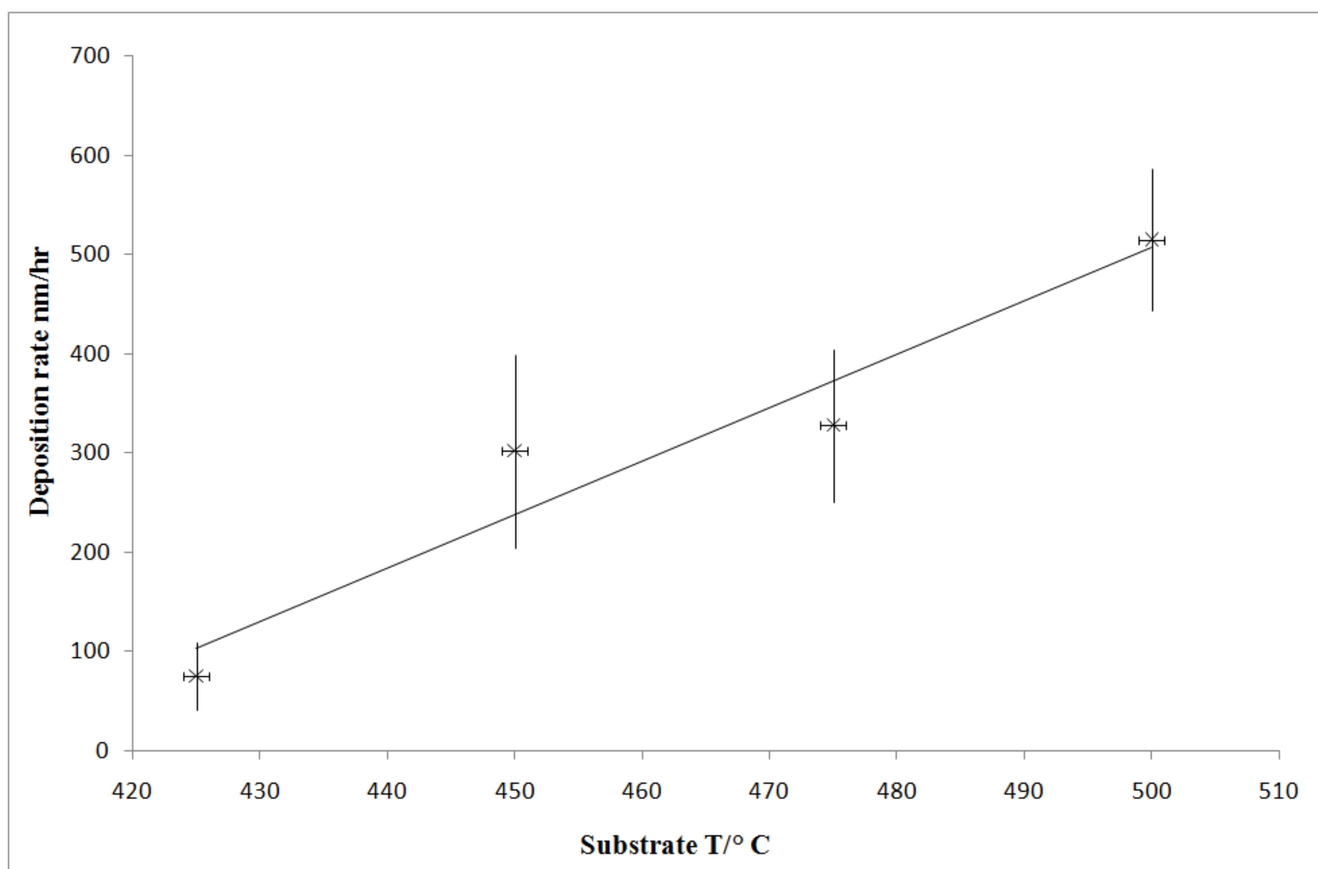

Figure 4 - Film growth rates as a function of substrate temperature

In comparison to the use of [Bi(mmp)$_3$] as a bismuth oxide precursor,[17] we did not observe constant/fixed film growth rates as a function of substrate temperature. The film thickness at substrate temperatures of 425 °C was approximately 75 nm, and at 500 °C approximately 520 nm. The deposition rates were therefore ca. 75 nm, 302 nm, 328 nm and 515 nm hr^{-1} at substrate temperatures of 425, 450, 475 and 500 °C respectively. Typically all deposited films demonstrated good substrate coverage and uniformity.

The top-down SEM micrographs of the deposited bismuth oxide films displayed a variety of morphologies according to temperature (Figure 5).

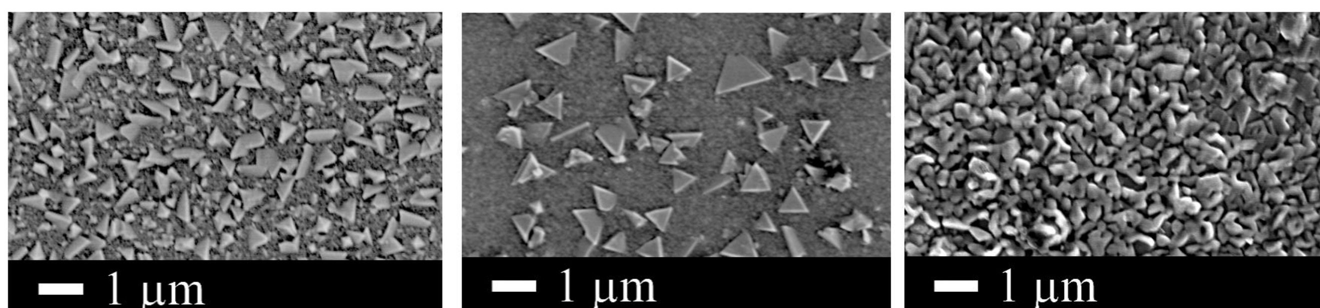

5 **Fig. 5**- Scanning electron micrographs of Bi_2O_3 films deposited via LPCVD of [Bi(O^{t}Bu)$_3$] at 425 °C (left), 475 °C (centre), and 500 °C (right).

Crystallites of varying size (0.4 – 2μm) are clearly observed in the SEM images, with profound triangular facets apparent in films deposited at 425 °C and 475 °C, and these facets are better defined at the higher temperature. 10 The film growth appeared to be non-uniform, particularly at 475 °C, however the film deposited at 500 °C displayed increased uniformity with the grains appearing to have coalesced. The optical properties of the deposited Bi_2O_3 films were measured using UV-vis spectroscopy in transmission mode. The band gap values obtained via Tauc plots[28] appear to be in general agreement with other bismuth oxide band gap values derived from similar experiments.[9,29] The band gap values of films possessing the β- phase as the dominant phase are in 15 the range 2.2 – 2.4 eV, with those predominantly γ- phase displaying band gaps between 2.7 – 3.0 eV and are in agreement with the literature.[10,30,31,39] The films described as mixed β- and γ- phase possessed band gaps in the region 2.3 – 2.6 eV.

Raman spectra were recorded for all of the bismuth oxide films grown via LPCVD of [Bi(O^{t}Bu)$_3$]. The predominantly β-Bi_2O_3 films exhibited few distinguishable features in the Raman spectrum. Broad peaks at 372 20 cm^{-1} and 580 cm^{-1} were the only two peaks observed with a relatively largebackground signal due to breakthrough to the substrate in these thin films. The Raman spectra of the predominantly γ-Bi_2O_3 film deposited at 500 °C (Figure 6) displayed peaks at 533, 452, 319, 279, 211, 154, 141 and 125 cm^{-1} which were identical to reported Raman spectra of the metal cation stabilised sillenite structures $Bi_{12}(Bi_{0.53}Mn_{0.47})O_{20}$ and $Bi_{12}SiO_{20}$[32] and $Bi_{12}TiO_{20}$,[33] the structures of which are all body-centred cubic and may be represented 25 parentally by γ-Bi_2O_3 with general structure $Bi_{12}(Bi_{4/5-n/x}M^{n+}{}_{5x})O_{19.2+nx}$,[34] however the peak at 185 cm^{-1} (Figure 6) remains unassigned.

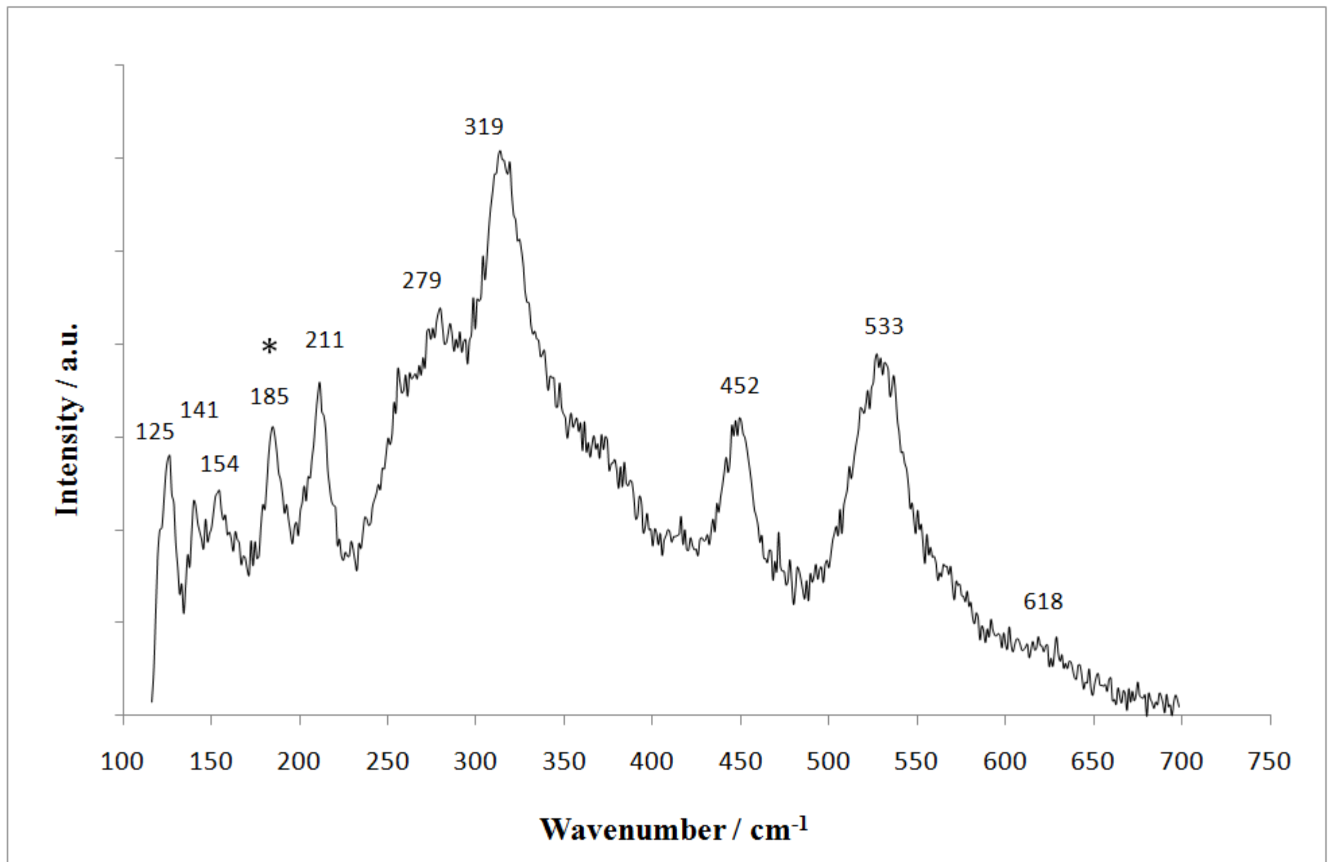

Fig. 6- Raman spectrum for the predominantly γ-Bi_2O_3 film deposited at 500 °C

The compositions of the as-deposited films were studied using X-ray Photoelectron Spectroscopy (XPS). The bismuth 4f surface ionisation displayed one principle environment, with the Bi $4f_{7/2}$ peak observed at 158.8 eV for all films, characteristic of Bi_2O_3.[35] The O 1s ionisation was observed between 529.7 – 529.8 eV, and such a position is characteristic of oxygen bound to bismuth in Bi_2O_3.[35] Bismuth to oxygen ratios close to Bi_2O_3 were observed for all films in the range 1.3 – 1.6 oxygen atoms to bismuth with oxygen deficient stoichiometries found for films deposited at 425 °C (1.4), 450 °C (1.4) and 500 °C (1.3). This is similar to reported XPS data[12] of β-Bi_2O_3 thin films, ascribed to the formation of oxygen-deficient β-Bi_2O_{3-x} as a result of oxygen vacancies found in the lattice. Etching experiments were carried out, however this resulted in preferential sputtering of lighter atoms, and exact bismuth and oxygen compositions could not be determined after etching. Carbon decreased dramatically after etching, suggesting that the carbon on the film surface is due to adventitious carbon contamination; however quantification in the bulk was not possible due to extreme distortion of the bismuth peak after etching.

Films deposited at 475 °C (band gap 2.3 eV) and 500 °C (band gap 2.8 eV) were chosen for an investigation into their water degradation properties under UV-light, the experimental details of which are described elsewhere.[36] In addition to the two Bi_2O_3 films, an uncoated borosilicate glass substrate was tested and used as a reference. After suspending each sample in the oxygen electrode chamber (consisting of a 0.1M KOH and 0.01M $Na_2S_2O_8$ solution previously purged with oxygen-free nitrogen), the sample was enclosed in the chamber

and irradiated with a 16 W, 365 nm UV-light for 1800 seconds from a distance of 50 mm. The generated dissolved oxygen concentration was plotted as a function of time, and the rate of oxygen production determined from the gradient of these plots (Table 2).

Table 2 - Summary of the individual film properties and the rate of oxygen production for the two films chosen

Substrate temp / °C	Film Thickness / nm	Bandgap / eV	Rate of O_2 production / μmol/hr
475	328	2.3	0.44
500	515	2.8	1.1
Uncoated Glass	-	-	0

Appreciable oxygen evolution was observed in the presence of UV-light for two samples of undoped Bi_2O_3 thin films, formed via LPCVD of [Bi(O^{t}Bu)$_3$], whereas the substrate-only experiment, which acted as a reference, exhibited zero oxygen production as expected.

Films deposited at 500 °C, which were predominantly γ- phase, resulted in 2.5 times the rate of oxygen evolution in comparison to films deposited at 475 °C, which were mixed β- and γ- phase, despite the latter sample possessing a narrower bandgap of 2.3 eV compared to 2.8 eV. The comparison of photocatalyst results obtained under different experimental conditions is notoriously difficult, as noted by Kudo and Miseki in their comprehensive review,[37] however the results obtained here for the photo-oxidation of water are of the order of those obtained from the use of optimised TiO_2 (anatase) thin films on glass investigated using an identical experiment, that yielded oxygen evolution rates between 0.056 – 0.440 μmol/hr.[36] An apparent quantum yield of 9.8% (at 365 nm) was calculated using Eqtn 1, which demonstrates these Bi_2O_3 films are at least as active as a range of oxide photocatalysts.[37]

$$\text{Apparent Quantum Yield } (\Phi_{O_2}) = \frac{4 \text{ x } O_2 \text{ rate } (\mu\text{mol/hr})}{\text{photon rate } (\mu\text{Einsteins/hr})}$$

This appears to be the first investigation into the water photodegradation properties of *undoped* Bi_2O_3 thin films synthesised by chemical vapour deposition. The hydrogen production from visible-light photocatalytic splitting of water has already been reported using bulk γ-Bi_2O_3 on Pt/RuO_2 (Φ_{H_2} = 1.1%)[38] and when using transition metal ion-doped γ-Bi_2O_3 (Φ_{H_2} = 1.3%).[39] Recent work[40] has shown that Pt-doped bulk α-Bi_2O_3 is able to degrade organic pollutants under visible light, so the potential for Bi_2O_3 induced photocatalysis is encouraging.

Conclusions

$[Bi(O^tBu)_3]$ has proved to be an excellent single-source precursor for MOCVD of crystalline Bi_2O_3 films at a variety of substrate temperatures, system pressures and carrier gas flow rates, with the relatively low bubbler temperatures required to transport the precursor through the system and clean decomposition to Bi_2O_3 giving it a distinct advantage over other commonly used bismuth precursors. The films consisted of variable mixtures of β- and γ- phases, but under particular conditions, the β- or γ- phases could be grown preferentially. All films possessed band gaps between 2.3 – 3.0 eV dependent upon the phase present. Top-down SEM imaging generally revealed an island-type growth mechanism with morphology varying with temperature. Film thickness increased with respect to substrate temperature and total system pressure. XPS conducted on the films chosen revealed an approximate 2:3 ratio of Bi:O, with carbon contamination decreasing dramatically upon etching. We have also demonstrated the use of these films for UV-light induced photodegradation of water into oxygen.

Acknowledgements

The EPSRC and UCL are thanked for a Studentship (SM). The Ramsay Memorial Fund is thanked for a Fellowship (GH). Thanks go to Dr S. Firth for assistance with DSC and Raman experiments, and to Mr K. Reeves for assistance with SEM measurements. Dr Emily Smith (University of Nottingham) is thanked for carrying out XPS analysis under EPSRC grant EP/F019750/1: "A Coordinated Open-Access Centre for Comprehensive Materials Analysis."

References

[1] B. H. Park, B. S. Kang, S. D. Bu, T. W. Noh, J. Lee and W. Jo, *Nature,* 1999, **401**, 682

[2] J. Wang, J. B. Neaton, H. Zheng, V. Nagarajan, S. B. Ogale, B. Liu, D. Viehland, V. Vaithyanathan, D. G. Schlom, U. V. Waghmare, N. A. Spaldin, K. M. Rabe, M. Wuttig and R. Ramesh, *Science,* 2003, **299**, 1719

[3] M. K. Singh, Y. Yang and C. G. Takoudis, *Coord. Chem. Rev.,* 2009, **253**, 2920

[4] C. Michel, M. Hervieu, M. M. Borel, A. Grandin, F. Deslandes, J. Provost and B. Raveau, *Z. Physik B - Condensed Matter,* 1987, **68**, 421

[5] A. M. Azad, S. Larose and S. A. Akbar, *J. Mater. Sci.,* 1994, **29**, 4135

[6] G. S. Devi, S. V. Manorama and V. J. Rao, *Sens. Actuators B – Chemical,* 1999, **56**, 98

[7] H. Heidong, Q. Wei,W. Xiaohong, D. Xianbo, C. Long and J. Zhaohua, *Thin Solid Films,* 2007, **515**, 5362

[8] K. Gurunathan, *Int. J. Hydrogen Energy,* 2004, **29**, 933

[9] L. Leontie, M. Caraman, M. Alexe and C. Harnagea, *Surf. Sci.*, 2002, **507**, 480

[10] L. Zhou, W. Wang, H. Xu, S. Sun and M. Shang, *Chemistry – A European Journal,* 2009, **15**, 1776

[11] L. Zhang, W. Wang, J. Yang, Z. Chen, W. Zhang, L. Zhou and S. Liu, *Appl. Catalysis A: General,* 2006, **308**, 105

[12] G. Bandoli, D. Barreca, E. Brescacin, G. A. Rizzi and E. Tondello, *Chem. Vap. Deposition,* 1996, **2**, 238

[13] C. Bedoya, G. G. Condorelli, G. Anastasi, A. Baeri, F. Scerra, I. L. Fragala, J. G. Lisoni and D. Wouters, *Chem. Mater.,* 2004, *16*, 3176

[14] C. Bedoya, G. Condorelli, S. T. Finocchiaro, A. DiMauro, I. L. Fragala, L. Cattaneo and S. Carella, *Chem. Vap. Deposition,* 2005, **11**, 261

[15] H. W. Kim, J. H. Myung and S. H. Shim, *Solid State Comm.,* 2006, **137**, 196

[16] H. W. Kim, J. H. Myung, S. H. Shim and C. Lee, *Appl. Phys. A* 2006, **84**, 187

[17] P. A. Williams, A. C. Jones, M. J. Crosbie.; P. J. Wright, J. F. Bickley, A. Steiner, H. O. Davies, T. J. Leedham and G. W. Critchlow, *Chem. Vap. Deposition,* 2001, **7**, 205

[18] T. Hatanpaa, M. Vehkamaki, M. Ritala and M. Leskela, *Dalton Trans.,* 2010, **39**, 3219

[19] S. W. Kang and S. W. Rhee, *Thin Solid Films,* 2004, **468**, 79

[20] M. Vehkamaki, T. Hatanpaa, M. Ritala and M. Leskala,. *J. Mater. Chem.,* 2004, **14**, 3191

[21] A. Haaland, H. P. Verne, H. V. Volden, R. Papiernik and L. G. Hubert-Pfalzgraf, *Acta. Chem. Scand.,* 1993, **47**, 1043

[22] C. S. Blackman, C. J. Carmalt, S. J. A. Moniz, S. E. Potts, H. O. Davies and D. Pugh, *ECS Trans*., 2009, **25**, 561

[23] M. C. Massiani, R. Papiernik, L. G. Hubert-Pfalzgraf and J-C Daran, *Polyhedron,* 1991, **10**, 437

[24] W. A. Hermann, N. W. Huber, R. Anwander and T. Priermeier, *Chem. Ber.,* 1993, **126**, 1127

[25] SAFC Hitech Ltd. Product Catalogue 2008, accessed 15 March 2010: *http://www.safcglobal.com/etc/medialib/docs/SAFC/Bulletin/product-catalogue-2008.pdf*

[26] Y. Kojima, H. Kadokura, Y. Okuhara, M. Matsumoto and T. Mogi, *Integrated Ferroelectrics,* 1997, **18**, 183

[27] H. A. Harwig, *Z. Anorg. Allg. Chemie,* 1978, **444**, 151

[28] J. Tauc, R. Grigorovici and A. Vancu, *physica status solidi (b).*, 1966, **15**, 627

[29] V. Dolocan, *Appl. Phys.,* 1978, **16**, 405

[30] B. L. Zhu and X. Z. Zhao, *Opt. Mater.,* 2006, **29**, 192

[31] P. Maruthamuthu, K. Gurunathan, E. Subramanian and M. V. C. Shastri, *Int. J. Hydrogen Energy,* 1993, ***18***, 9

[32] B. Mihailova, M. Gospodinov and L. Konstantinov, *J. Phys. Chem. Sol.,* 1999, **60**, 1821

[33] B. Mihailova, G. Bogachev, V. Marinova and L. Konstantinov, *J. Phys. Chem. Sol.,* 1999, **60**, 1829

[34] M. Valant and D. Suvorov, *Chem. Mater.,* 2002, **14**, 3471

[35] V. S. Dharmadhikari, *J. Electron Spec.,* 1982, **25**, 181

[36] G. Hyett, J. A. Darr, A. Mills and I. P. Parkin, *Chemistry – A European Journal,* 2010, accepted for publication

[37] A. Kudo, Y. Miseki, *Chem. Soc. Rev.*, 2009, **38**, 252

[38] P. Maruthamuthu, K. Gurunathan, E. Subramanian and M. V. C. Shastri, *Int. J. Hydrogen Energy,* 1994, **19**, 889

[39] K. Gurunathan, *Int. J. Hydrogen Energy,* 2004, **29**, 933

[40] R. Li, W. Chen, H. Kobayashi and C. Ma, *Green Chem.,* 2010, **12**, 212